ACS APPLIED MATERIALS & INTERFACES

Research Article

www.acsami.org

Liquid-Crystalline Blue Phase II System Comprising a Bent-Core Molecule with a Wide Stable Temperature Range

Kyung-Won Park, Min-Jun Gim, Sunhwan Kim, Sung-Taek Hur, and Suk-Won Choi*

Department of Advanced Materials Engineering for Information and Electronics and Regional Innovation Center, Components and Materials for Information Displays, Kyung Hee University, Yongin, Gyeonggi-do 446-701, South Korea

Supporting Information

ABSTRACT: A thermodynamically stable blue phase II (BPII) has been prepared, and its electrooptical (EO) performance has been evaluated in a host system of a conventional rodlike nematogen mixed with a bent-core molecule. For the mixed system presented, the widest temperature range of BPII stability, during cooling/heating, was >6 °C. This range is much wider than those of conventional nematogens blended with chiral dopants. EO observations show that the BPII produced exhibited stable EO performance based on the EO Kerr effect. The temperature dependence of the Kerr effect was found to be in approximate agreement with the Landau−de Gennes theory. Furthermore, this material demonstrated very fast, sub-millisecond-scale, response times, thus showing potential for use in high-speed EO devices.

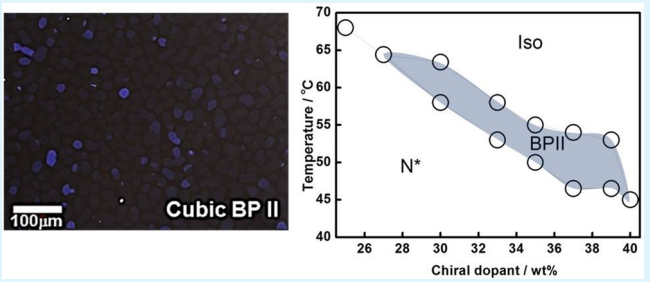

KEYWORDS: *liquid-crystalline blue phase, electrooptical Kerr effect, bent-core molecule, nematogen*

1. INTRODUCTION

Liquid crystals (LCs) are a class of soft materials formed by nanoscale molecular self-assembly. They exist as various phases that are stable at different temperature ranges. Among the several liquid-crystalline phases, the blue phase (BP), which exists in a temperature range intermediate to those of the low-temperature chiral nematic (N*) and high-temperature isotropic phases, has attracted significant research interest. This interest is a result of its unusual three-dimensional (3D) nanostructure, which forms spontaneously and has great potential for application in advanced optical devices, such as fast optical shutters and tunable photonic crystals.[1] BPs have a double-twisted cylinder (DTC) structure, the self-assembly of which, in 3D space, determines their unique nanostructure.[1] BPs can be classified into two broad categories, namely, cubic and amorphous BPs, in order of increasing temperature.[2,3] Furthermore, cubic BPs can be classified into two categories, namely, a body-centered-cubic BP (BPI) and a simple cubic BP (BPII), in order of increasing temperature.[1] In contrast, amorphous BP, referred to as BPIII, is believed to consist of DTCs of arbitrary orientation. Hence, BPIII materials are regarded as having isotropic symmetry.[4] In general, each BP is stable in a narrow temperature range, typically 0−1 °C, which limits their utility in electrooptical (EO) devices. This limitation could be overcome if the temperature range of their stability was increased to 60 °C or more including room temperature. The formation of polymer-stabilized BP materials offers a means to this goal.[5]

On the other hand, pure cubic BPs with temperature ranges of more than 10 °C have been reported to have been fabricated using achiral bent-core molecular systems, without polymer stabilization.[6−8] It has been suggested that biaxiality,[9,10] flexoelectricity,[11] and an elastic constant[7,12] are crucial elements of the stabilization mechanisms of these systems. Because bent-core molecules possess all of these desirable features, they are promising molecules for stabilizing cubic BPs.[13,14] Nevertheless, details of the EO performances of pure BPs stabilized by bent-core molecules have been scarcely reported.[6,15] We attribute this to the fact that, although it expands the stable temperature ranges of BPs, incorporation of bent-core molecules usually hinders the EO performance. Moreover, EO performances of BPII materials in these mixed systems have, to date, not been reported because their temperature ranges are extremely narrow.

In this work, we prepared a clearly distinguishable BPII material, comprised of a mixture of a conventional rodlike nematogen and an intriguing bent-core molecule, which is stable over a wide temperature range (>6 °C). After many trials of combining conventional rodlike nematogens with bent-core molecules, we discovered a mixture that would produce BPII. To the best of our knowledge, although bent-core molecule-based BPI and BPIII systems possessing wide temperature ranges upon cooling have been reported by several research groups,[6−8] such a wide range of BPII stability upon heating, as is presented here, has not been reported previously. In addition, we performed an in-depth analysis on the EO performance of

Received: June 1, 2013
Accepted: August 2, 2013
Published: August 2, 2013

the cubic BPII prepared in this study. The prepared BPII was observed to be thermodynamically stable and to demonstrate a large EO Kerr effect. Ultimately, this work demonstrates the potential for liquid-crystalline BPII materials to be used in high-speed EO devices based on the EO Kerr effect.

2. EXPERIMENTAL SECTION

Figure 1a presents the chemical structure of the bent-core molecule used. This molecule was first reported by Weissflog et al.[16] It exhibits

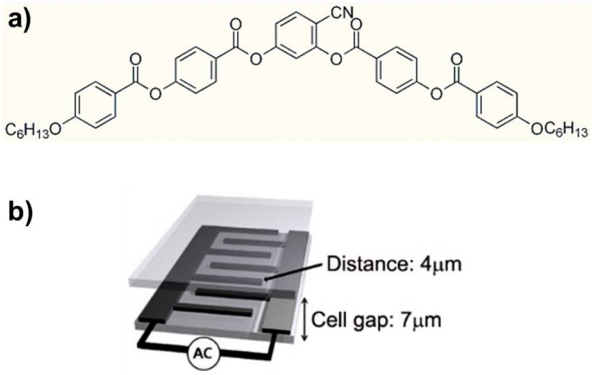

Figure 1. (a) Chemical structure of the bent-core molecule used in this work. (b) Structure of a sandwiched cell with comb-type interdigitated electrodes.

the following phase formation sequence during cooling: isotropic−140 °C−nematic−105 °C−crystalline. The nematic phase of this bent-core molecule can be regarded as a positive LC, having a positive dielectric anisotropy ($\Delta\varepsilon$ = +2.12 at 130 °C).

A host mixture (BC10), consisting of 90 wt % conventional rodlike nematic LCs (BYLC53XX, BaYi Space Co.) and 10 wt % bent-core molecules, was prepared. The prepared BC10 host mixture had a positive $\Delta\varepsilon$ and showed the following phase sequence during cooling: isotropic−100 °C−nematic−45 °C−crystalline. Experimental $\Delta\varepsilon$ and birefringence (Δn) values of BC10, as a function of the temperature, are described in the Supporting Information. In order to introduce chirality into host mixtures, a commercially available chiral dopant (R811, Merck) was blended using concentrations ranging from 25 to 40 wt %.

For polarizing optical microscopy (POM) observations, mixtures were injected into 5-μm-thick cells without any surface treatment such as rubbing.

In order to evaluate the EO performance, sandwich cells with comb-type interdigitated electrodes were fabricated on only the bottom substrate, as shown in Figure 1b. The distance between the electrodes was 4 μm. No surface treatment was performed on the substrate, and the cell gap between the two substrates was maintained using 7-μm-thick film spacers. A 1 kHz square-wave root-mean-square (rms) voltage was employed to test the samples. The transmittance was normalized to that of the cell when it was in an isotropic state and the two polarizers were in a parallel position.[4] The response time was measured using a 1 kHz square-wave voltage between 0 and 40 V_{rms} μm^{-1}.

3. RESULTS AND DISCUSSION

3.1. Temperature Range of BPs. First, we checked for the possibility of BP emergence from the pure nematic LC containing no added bent-core molecule. We confirmed that BP did not appear in the pure nematic LC using several concentrations of the chiral dopant. BP only appeared in mixtures consisting of both the nematic LC and bent-core molecule. Figure 2 illustrates a sequence of typical POM images, revealing the textures of a chiral mixture composed of BC10 blended with 37 wt % chiral dopant. Upon cooling at a rate of 0.1 °C min^{-1}, the isotropic liquid changed to a dark fluid phase. This phase appeared to be comprised of platelets, which are usually observed in cubic BPII, as shown in Figure 2a. Upon further cooling, BPII progressed to another BP phase (BPI), as shown in Figure 2b, followed by a N* phase, shown in Figure 2c.

To understand precisely the phase transition between BPII and BPI upon cooling, the temperature dependence of the Bragg reflection from the mixture was investigated. Figure 3 illustrates the typical temperature dependence of the Bragg reflection wavelength of a mixture of BC10 blended with 37 wt % chiral dopant. Figure 3a clearly shows a discontinuous change in the temperature dependence of the Bragg reflection wavelength at the BPII−BPI transition during cooling (0.1 °C min^{-1}). Reflections in the temperature regions above and below the transition point are associated with the (100) and (110) reflections of the cubic lattice vectors of nanostructured BPII and BPI, respectively.[17,18] The Bragg reflection wavelength shifted by ~60 nm from 410 to 470 nm during the transition from BPII to BPI. From POM and Bragg reflection observations, it was apparent that the chiral mixture prepared in this study possessed both BPII and BPI during the cooling process. Furthermore, the temperature dependence of the Bragg reflection wavelength during heating (0.1 °C min^{-1}) was also recorded, as shown in Figure 3b. During heating, no meaningful reflection wavelength could be observed at temperatures of <46 °C. This is attributed to the chiral pitch (<400 nm) being too short to produce the precise Bragg reflection at wavelengths detectable by our experimental setup. POM observations indicated that the phase present at temperatures of <46 °C was the N* phase. The BPI, which

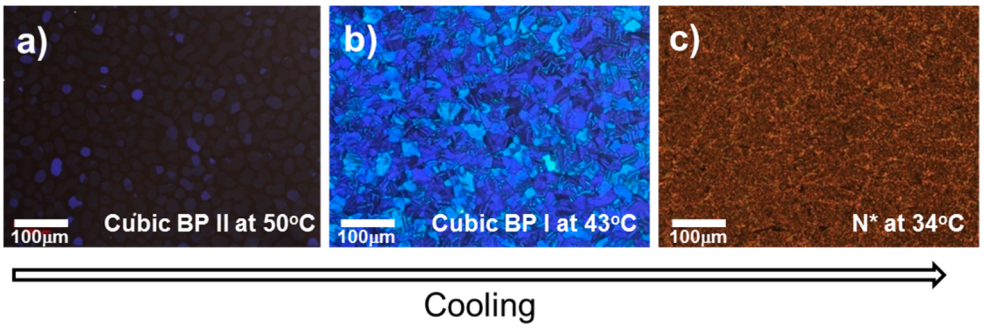

Figure 2. Typical POM images revealing the textures of chiral mixtures composed of BC10 blended with 37 wt % chiral dopant: (a) cubic BPII at 50 °C; (b) cubic BPI at 43 °C; (c) N* at 34 °C.

dx.doi.org/10.1021/am403109q | ACS Appl. Mater. Interfaces 2013, 5, 8025−8029

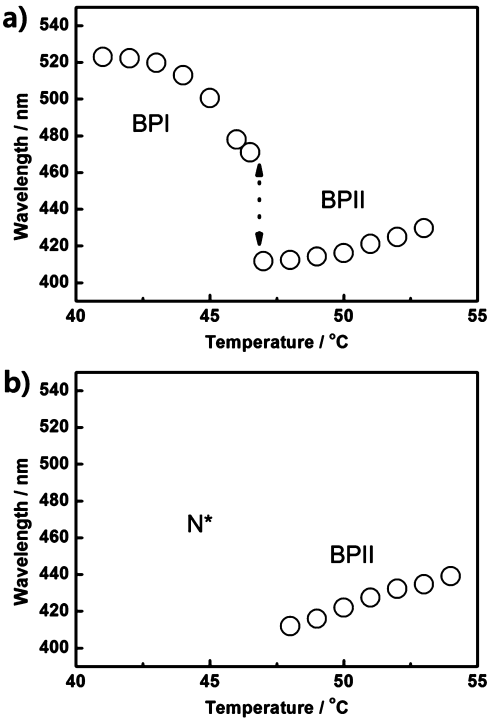

Figure 3. Temperature dependence of the Bragg reflection wavelength during (a) cooling and (b) heating at 0.1 °C min^{-1}.

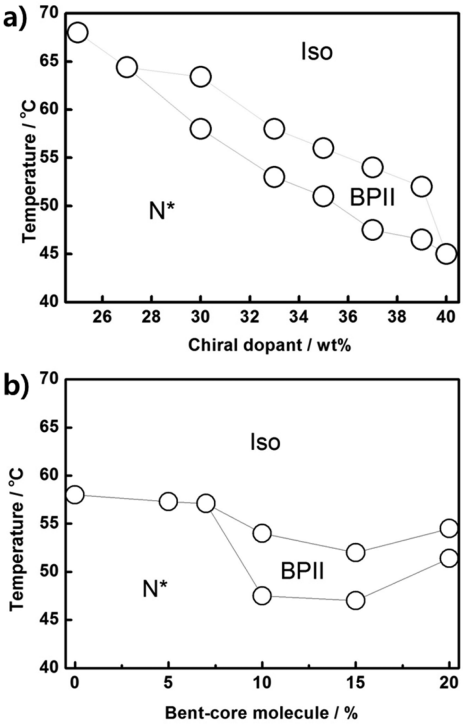

Figure 4. Phase diagram obtained by heating for (a) BC10 as a function of the chiral content and (b) several host nematic LC mixtures doped with 37 wt % chiral dopant as a function of the bent-core molecule concentration.

appeared at a lower temperature range upon cooling, was not observed upon heating. Thermodynamic equilibrium phase-transition points are better reflected during heating than cooling because supercooling occurs readily upon cooling.[19] Thus, the BPI observed in our system during cooling was a result of supercooling. However, at temperatures of >46 °C, the Bragg reflection wavelength gradually increased with the temperature. This trend corresponds well with that observed for BPII during cooling. Consequently, the BPII observed in this work is known to be thermodynamically stable because it appeared during both cooling and heating.

On the basis of POM results and Bragg reflection observations, we have produced a phase diagram (Figure 4a) for BC10 as a function of the chiral content, using a heating rate of 0.1 °C min^{-1}. In addition, Figure 4b shows a phase diagram for several host nematic LC mixtures, doped with 37 wt % chiral dopant, as a function of the bent-core molecule concentration, also obtained at a heating rate of 0.1 °C min^{-1}. In our mixed system, the temperature range of BPII increased to >6 °C at its widest during the heating process, which was much wider than that of conventional nematogens blended with chiral dopants. Unfortunately, we cannot yet explain why BPII was stable in our mixed system. Further investigation is needed to describe this mechanism.

3.2. EO Performance. Typical POM images, corresponding to the extremes of the applied electric fields, of our BPII (49.5 °C) in a chiral mixture composed of BC10 blended with 37 wt % chiral dopant are shown in Figure 5a. The normally black state gradually brightened and finally turned completely white under the crossed-polarizer conditions of the POM. Upon removal of the applied electric field, the BPII reverted to being black. Figure 5b illustrates a typical voltage−transmittance (V−T) curve for the BPII at 49.5 °C. The transmittance gradually increased with the applied voltage. With decreasing applied voltage, the V−T curve overlapped well with that of the

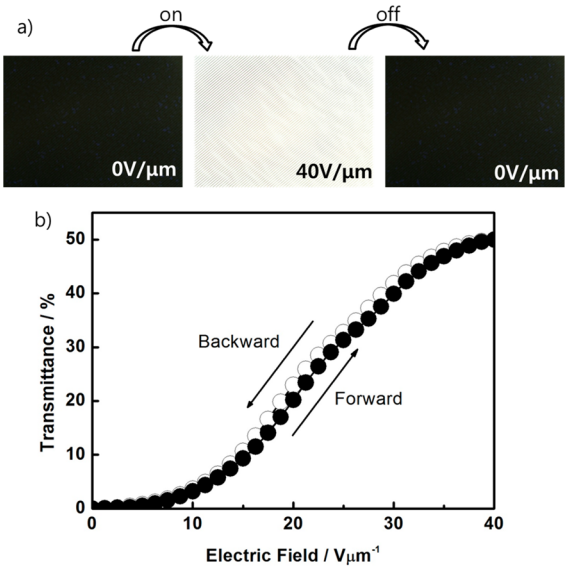

Figure 5. (a) Typical POM images of the BPII produced, obtained at maximum and minimum applied electric field voltages. (b) Typical V−T curves of our BPII system.

increasing voltage, as shown in Figure 5b. Even after repeated evaluations, very little hysteresis was observed.

The response time of the BPII was also measured in a chiral mixture composed of BC10 blended with 37 wt % chiral dopant. A typical response profile of the BPII at 49.5 °C is presented in Figure 6a. The temperature dependence of the rise and decay times of BPII is shown in Figure 6b. Over a temperature range from 47.1 to 53.5 °C, BPII response times were on the order of sub-milliseconds. This is much shorter

dx.doi.org/10.1021/am403109q | ACS Appl. Mater. Interfaces 2013, 5, 8025−8029

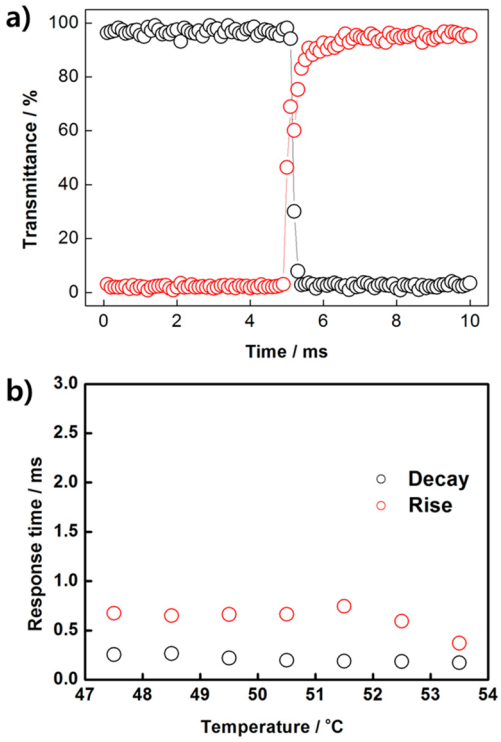

Figure 6. (a) Typical response profile for the BPII produced. (b) Temperature dependence of the rise and decay times of our BPII system.

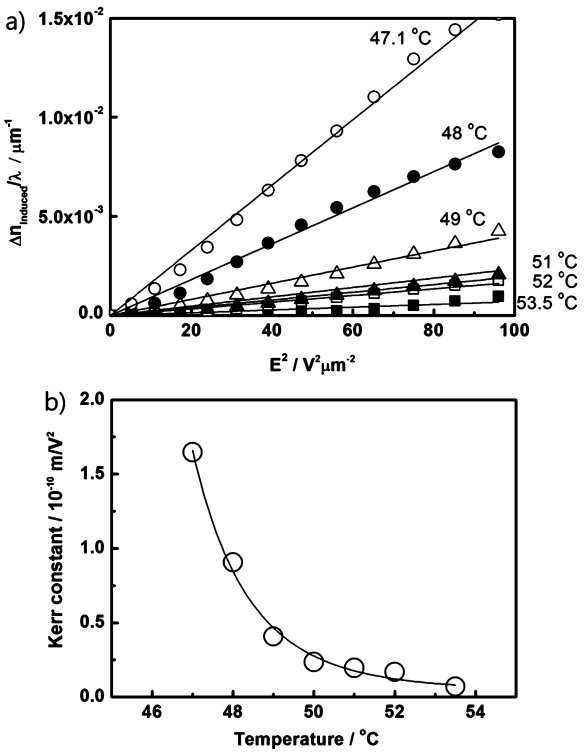

Figure 7. (a) Plot of $\Delta n_{induced}/\lambda$ of BPII as a function of E^2, measured at several temperatures. The solid curve is a fit based on the Landau–de Gennes theory. (b) Measured Kerr constants of BPII as a function of the temperature.

than those of nematic LCs, which generally range from approximately 10 ms to several tens of milliseconds. In general, decay times are longer than rise times for conventional nematic LCs. Slow decay response is a critical problem for conventional LC devices because the decay response relies solely on an LC's material properties, irrespective of the voltage applied.[20] However, we observed decay times comparable to rise times in this system. Such fast decay responses are characteristic of short correlation lengths and large elastic resistances in BPII.

By comparing the $V-T$ curves of our BPII to those of the conventional BPI, reported previously,[4,21] we found that our BPII exhibited a lower transmittance, higher operating transmittance, and much less hysteresis. These differences are attributed to the influence of structural differences in the DTCs and defect lines between BPI and BPII. In addition, although a hysteresis-free amorphous BPIII has been reported,[22] our BPII demonstrates a faster response time owing to its shorter correlation length.

Figure 7a shows a plot of $\Delta n_{induced}/\lambda$ for BPII as a function of the square of the applied electric field (E^2), measured at several temperatures in a chiral mixture composed of BC10 blended with 37 wt % chiral dopant. Here, $\Delta n_{induced}$ denotes the induced birefringence, λ signifies the wavelength of the probe light, and E refers to the applied electric field. A helium–neon laser (633 nm) was employed as the probe light in this work. As shown in Figure 7a, although deviations from linearity were observed when stronger electric fields were applied, it is clear that $\Delta n_{induced}/\lambda$ is approximately proportional to E^2. This EO phenomenon is known as the Kerr effect,[23] a second-order nonlinear EO effect expressed as follows:

$$\Delta n_{induced} = \lambda K E^2 \quad (1)$$

The proportionality constant, calculated from the slope of the linear function between $\Delta n_{induced}/\lambda$ and E^2, indicates the Kerr constant (K). K in BPII can also be described as a function of the temperature, as shown in Figure 7b. From our investigation, the temperature dependence of the Kerr effect for BPII was found to be in approximate agreement with the Landau–de Gennes theory.[24] K of BPII spanned orders of magnitude (10^{-11}–10^{-10} m V^{-2}) over the temperature range studied. These values are 10–100 times greater than those of conventional Kerr materials such as nitrobenzene, which is known to have a very large Kerr constant ($K = 2.2 \times 10^{-12}$ m V^{-2}).[25,26] However, the observed K of our BPII is similar to those of BPI and BPIII materials previously reported by other research groups.[15,27]

4. CONCLUSION

We have successfully prepared a thermodynamically stable BPII and evaluated its EO performance in a host mixture comprised of a conventional rodlike nematogen and a bent-core molecule. Surprisingly, in our mixed system, the widest stable temperature range observed for BPII was increased to >6 °C during cooling/heating. From EO observations, it was shown that this BPII exhibits a stable EO performance based on the EO Kerr effect. In addition, the temperature dependence of the Kerr effect for this BPII was found to be in approximate agreement with the Landau–de Gennes theory. Furthermore, very fast response times were observed. From an application perspective, the temperature range of the BPII should be larger than that of the BPII material studied here. Thus, our future goal is to enhance the temperature range of BPII, through polymer stabilization, to >60 °C, including room temperature. In

dx.doi.org/10.1021/am403109q | ACS Appl. Mater. Interfaces 2013, 5, 8025–8029

addition, we will work toward developing BPII materials with much larger K than that of the BPII obtained in this work.

■ ASSOCIATED CONTENT

Supporting Information

$\Delta\varepsilon$ and Δn of the BC10 as a function of the temperature. This material is available free of charge via the Internet at http://pubs.acs.org.

■ AUTHOR INFORMATION

Corresponding Author

*E-mail: schoi@khu.ac.kr.

Notes

The authors declare no competing financial interest.

■ ACKNOWLEDGMENTS

This work was supported by the National Research Foundation of Korea grant funded by the Ministry of Science, ICT & Future Planning (Grant 2012R1A2A2A06046931).

■ REFERENCES

(1) Kikuchi, H. *Struct. Bonding (Berlin)* **2008**, *128*, 99.
(2) Gim, M.-J.; Hur, S.-T.; Park, K.-W.; Lee, M.; Choi, S.-W.; Takezoe, H. *Chem. Commun.* **2012**, *48*, 9968−9970.
(3) Hur, S.-T.; Lee, B. R.; Gim, M. J.; Park, K. W.; Song, M. H.; Choi, S.-W. *Adv. Mater.* **2013**, *25*, 3002−3006.
(4) Chen, K.-M.; Gauza, S.; Xianyu, H.; Wu, S.-T. *J. Disp. Technol.* **2010**, *6*, 318−322.
(5) Kikuchi, H.; Yokota, M.; Hisakado, Y.; Yang, H.; Kajikawa, T. *Nat. Mater.* **2002**, *1*, 64−68.
(6) Lee, M.; Hur, S. T.; Higuchi, H.; Song, K.; Choi, S.-W.; Kikuchi, H. *J. Mater. Chem.* **2010**, *20*, 5813−5816.
(7) Hur, S.-T.; Gim, M.-J.; Yoo, H.-J.; Choi, S.-W.; Takezoe, H. *Soft Matter* **2011**, *7*, 8800−8803.
(8) Zheng, Z.; Shen, D.; Huang, P. *New J. Phys.* **2010**, *12*, 113018.
(9) Wright, D. C.; Mermin, N. D. *Rev. Mod. Phys.* **1989**, *61*, 385.
(10) Yoshizawa, A.; Kogawa, Y.; Kobayashi, K.; Takanishi, Y.; Yamamoto, J. *J. Mater. Chem.* **2009**, *19*, 5759−5764.
(11) Castles, F.; Morris, S. M.; Terentjev, E. M.; Coles, H. *Phys. Rev. Lett.* **2010**, *104*, 157801.
(12) Alexander, G. P.; Yeomans, J. M. *Phys. Rev. E: Stat., Nonlinear, Soft Matter Phys.* **2006**, *74*, 061706.
(13) Jeong, H.-J.; Le, K. V.; Gim, M.-J.; Hur, S.-T.; Choi, S.-W.; Araoka, F.; Ishikawa, K.; Takezoe, H. *J. Mater. Chem.* **2012**, *22*, 4627−4630.
(14) Nakata, M.; Takanishi, Y.; Watanabe, J.; Takezoe, H. *Phys. Rev. E: Stat., Nonlinear, Soft Matter Phys.* **2003**, *68*, 041710.
(15) Le, K. V.; Aya, S.; Sasaki, Y.; Choi, H.; Araoka, F.; Ema, K.; Mieczkowski, J.; Jakli, A.; Ishikawa, K.; Takezoe, H. *J. Mater. Chem.* **2011**, *21*, 2855−2857.
(16) Kovalenko, L.; Schroder, M. W.; Reddy, R. A.; Diele, S.; Pelzl, G.; Weissflog, W. *Liq. Cryst.* **2005**, *32*, 857−865.
(17) Choi, H.; Higuchi, H.; Kikuchi, H. *Appl. Phys. Lett.* **2011**, *98*, 13905.
(18) Coles, H.; Pivnenko, M. *Nature* **2005**, *436*, 997−1000.
(19) Shibayama, S.; Higuchi, H.; Okumura, Y.; Kikuchi, H. *Adv. Funct. Mater.* **2013**, *23*, 2387−2396.
(20) Choi, S.-W.; Yamamoto, S.; Iwata, T.; Kikuchi, H. *J. Phys. D: Appl. Phys.* **2009**, *42*, 112002.
(21) Chen, Y.; Wu, S. T.; Yamamoto, S.-I.; Haseba, Y. *Appl. Phys. Lett.* **2013**, *102*, 141116.
(22) Yoshizawa, A.; Kamiyama, M.; Hirose, T. *Appl. Phys. Exp.* **2011**, *4*, 101701.
(23) Kerr, J. *Philos. Mag.* **1875**, *50*, 337.
(24) de Gennes, P. G.; Prost, J. *The Physics of Liquid Crystals*, 2nd ed.; Oxford University Press: Oxford, U.K., 1993.
(25) Hecht, E. *Optics*, 2nd ed.; Addison-Wesley Publishing Company: Reading, MA, 1987.
(26) Hisakado, Y.; Kikuchi, H.; Nagamura, T.; Kajiyama, T. *Adv. Mater.* **2005**, *17*, 96−98.
(27) Wang, L.; He, W.; Xiao, X.; Yang, Q.; Li, B.; Yang, P.; Yang, H. *J. Mater. Chem.* **2012**, *22*, 2383−2386.